DLSU RESEARCH CONGRESS 2023
MANILA, PHILIPPINES
JULY 5-7, 2023
Fostering a Humane and Green Future:
Pathways to Inclusive Societies and Sustainable Development

Clay-filled Polystyrene Coating Dispersed in D-limonene for Anti-corrosion Application

Aaron Ogrimina[1,#], Allison Jade Sia[1,#], Michael Dominic Ajero[1], Michelle Natividad[2], and David Penaloza Jr.[1,*]

[1] *Department of Chemistry, College of Science, De La Salle University Manila*
[2] *Department of Physics, College of Science, De La Salle University Manila*
**Corresponding Author: david.penaloza.jr@dlsu.edu.ph*
[#]Authors contributed equally

Abstract: Due to the various adverse effects that corrosion imposes, it is imperative to explore studies that center on developments and modifications of organic coating systems as a preventive measure. Polystyrene (PS) has potential as a polymer coating but its barrier and mechanical characteristics can still be further optimized by introducing an organically-modified nanoclay such as Cloisite-20 A (C20A). In this work, an environment-friendly and corrosion-resistant PS-based coating was synthesized through solution-casting with C20A using D-limonene as a green solvent. Formulations of C20A of varying concentrations (1-, 3-, and 5-wt%) were prepared and applied on galvanized metal coupons. The coated coupons were characterized through contact angle measurement, immersion test, and adhesion test and were compared to a commercial epoxy primer. Results showed that the contact angle of the PS-based coating decreased with the addition of C20A which increases in increasing concentration. On the other hand, the immersion test revealed that the corrosion rate and corrosion inhibition efficiency of 5% C20A, 0.02326 mm y^{-1}, and 65.88%, respectively, were significantly better than the other treatments including the PS-only coating and commercial epoxy primer after subjecting to analysis of variance (ANOVA) at 95% confidence level. The adhesion test revealed that 5% C20A has excellent adhesion comparable to that of the commercial sample while the PS-only coating exhibited poor adhesive properties. The corrosion inhibition performance of the 5% C20A can be attributed to the strong adhesion properties and improved barrier characteristics of the PS-based coating via the dispersion of C20A to the polymer matrix.

Key Words: corrosion rate; nanoclay; polystyrene coating; immersion test; solution-casting

1. INTRODUCTION

According to Ahmad (2006), corrosion is the deterioration of a material due to an electrochemical reaction with chemical or biological agents in the environment which poses serious adverse consequences. Corrosion costs approximately $2.5 trillion annually in addition to costs from product loss or contamination, storage leaks, and loss of material efficiency (Procopio, 2019; Ahmad, 2006). However, despite being unavoidable, it is preventable through coating systems.

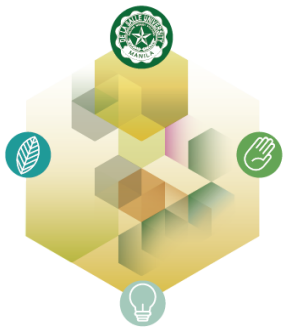

The basic purpose of coating systems for metal substrates is to isolate the metal surface from the corrosive environment (Schweitzer, 2006). To prolong the service life of the coating, excellent chemical properties are imperative which consist of optimized barrier characteristics, strong adhesion, coating homogeneity, and increased surface hydrophobicity.

Organic coatings have attracted interest for corrosion protection due to being low cost and efficient; however, due to inherent porosity, it is vulnerable to penetration of corrosive species (Nazari et al., 2022). The implementation of coating modification through nanomaterials gained interest in enhancing the barrier properties of coatings.

PS is a thermoplastic mass-produced through the catalytic dehydrogenation of ethylbenzene (Kik, Bukowska, & Sicińska, 2020). Due to its low cost and versatility, it is widely applicable for the production of compact disks, food packaging, and electronic parts (Kik, Bukowska, & Sicińska, 2020; Regalado, Punzalan, & Penaloza, 2018; Ho, Roberts, & Lucas, 2017). However, massive amounts of plastic accumulated due to commercialization led to an environmental concern due to its low biodegradability. In 2017, 26.28 million tons of PS was produced (Geyer, 2020). But recent studies have suggested the use of essential oils as shrinking agents to recycle waste PS products (García et al., 2009; Shikata et al., 2011). PS also has wide applications in nanocomposite research especially with clay and carbon nanotubes due to its improved mechanical and thermal properties (Amr et al., 2011; Fu & Qutubuddin, 2000).

Limonene, 1-methyl-4-(1-methyl phenyl) cyclohexene, is a colorless liquid with a citrusy aroma and taste (National Center for Biotechnology Information, 2022). Limonene has a wide range of applications in cosmetics, the food industry, and pharmaceuticals which it owes to its expansive properties (Ravichandran et al., 2018; Akhavan-Mahdavi et al., 2022). Furthermore, limonene is the most extensively researched terpene used for the environment-friendly recycling of PS due to its natural abundance and good biodegradability giving rise to many applications, particularly for polymer coating (Gil-Jasso et al., 2019; Regalado, Punzalan, & Penaloza, 2018).

C20A is a modified organophilic phyllosilicate resulting from the introduction of a quaternary ammonium salt to montmorillonite (MMT) clay (Firdaus et al., 2021). As an additive, an optimum 1-5% dispersion of this nanofiller in thermoplastics improves mechanical and barrier properties by improving the homogeneity between the silicate layers of the clay and the polymer matrix of the thermoplastic (Naderi-Samani et al, 2019; Firdaus et al, 2021; Sales et al., 2015; Dimitry et al., 2016). As a result of these improved properties, thermoplastic compounds benefit from increased adhesion strength, tensile modulus, and anti-corrosion properties (Naderi-Samani et al., 2019; Firdaus et al. 2021; Sales et al; 2015)

In this work, an environment-friendly and corrosion-resistant polymer coating was prepared via solution-casting of PS in D-limonene enhanced with C20A. PS has potential as a polymer coating but due to its poor barrier properties, optimization through the addition of C20A organoclay is ideal. And the use of D-limonene as an organic dispersing medium to dissolve PS allows for its application as a green solvent and poses a potential use for waste PS. The coatings were characterized through a contact angle measurement, immersion test, and adhesion test and was compared to the PS-only coating (negative control) and a commercial epoxy primer (positive control).

2. METHODOLOGY

2.1 Materials and reagents

PS pellets ($[CH_2CH(C_6H_5)]_n$; average M_w ~350 kDa) and 97% D-limonene ($C_{10}H_{16}$) were obtained from Sigma-Aldrich. C20A was procured from BYK-Chemie. Sodium chloride (NaCl) was obtained from UNI-CHEM. Sodium hydroxide (NaOH) was secured from Dalkem Corporation. Zinc metal powder (Zn) was acquired from HiMedia Laboratories Limited. A two-component epoxy-based primer with corrosion resistance properties was purchased from a local hardware store to serve as the commercial sample.

2.2 Sample Preparation

2.2.1 Synthesis

PS pellets were added in D-limonene to achieve 9-wt% PS [PS(9)] with respect to the D-limonene formulation. The PS was fully dispersed by magnetic stirring at 50 °C. From the base formulation of PS in D-limonene, C20A was incorporated in the following weight percentages (%wt) with respect to the PS/D-limonene dispersion: 1% C20A [C20A(1)], 3% C20A [C20A(3)], 5% C20A [C20A(5)].

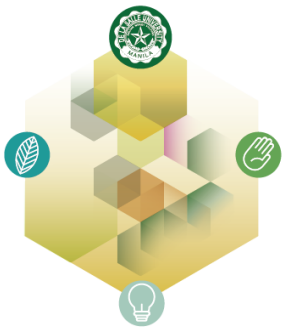

Once the corresponding weight of components was added to the PS/D-limonene dispersion, the formulations were mixed with a magnetic stirrer at 50 ºC, sonicated at 25 ºC, then stirred once more under the same previous settings.

2.2.2 Substrate preparation

The metal substrate used in the study is a 0.55 mm thick galvanized steel sheet cut into small rectangular coupons (38.1 mm × 25.4 mm) for the contact angle measurement and immersion testing and into the dimensions 76.2 mm × 50.8 mm × 0.55 mm for adhesion test. The surfaces of the metal panel were mechanically polished in succession using silicon carbide papers of 320-, 600-, and 1000-grit and cleaned using a paper towel. The mass of the bare metal coupons was obtained and recorded.

2.2.3 Coating application

The metal coupons were laid flat on a horizontal surface and the coating treatments were prepared. Three replicates of metal panels were coated with each treatment leaving three uncoated panels as blank samples. Three layers of the coating were applied on each side of the metal coupons and were cured at ambient temperature for 120 h. The coated panels were weighed, and the dry film thickness was about 1-3 mils measured using Mileseey Coating Thickness Gauge MC996 prior to any analysis.

2.3 Coating characterization

2.3.1 Contact angle measurement

Prior to the immersion test, the contact angle was determined according to ASTM D7334-08. A five µL drop of distilled water was deposited on three different points at the center of the metal panels using a Hamilton® 701N syringe. The image of the sessile drops was rapidly captured, and the contact angle was examined using ImageJ Low-Bond Axisymmetric Drop Shape Analysis. The contact angles for the treatments were analyzed using ANOVA at a 95% confidence interval (CI) on Statistica.

2.3.2 Immersion test

Each metal panel was submerged in separate 160 mL solutions of simulated seawater (3.5 wt% NaCl, pH 8.00-8.10). After 745 to 747 hours, the samples were removed and corrosion product removal was performed according to ASTM G1 using a mixture of NaOH, granulated Zn, and distilled water. The corroded metal coupons were ultrasonically immersed in this mixture for 30-40 minutes at 60ºC followed by removal of loose coating, rinsing with distilled water, and oven-drying for 30 minutes at 60ºC with no airflow. The corrosion rate and corrosion inhibition efficiency of the samples were quantitatively determined after weighing corroded panels from immersion testing and using ANOVA.

2.3.3 Cross-hatch adhesion test

The adhesion of the coatings was done in duplicates and through a cross-hatch adhesion test according to ASTM D3359-17. A 2mm11 multi-tip blade was used to make a cut through the cured coating film in two perpendicular directions to create a 10×10 lattice pattern. After lightly brushing the coating film, the center of the tape was placed on the grid and was firmly rubbed with an eraser to ensure good contact. Within 90±30 s of application, the tape was rapidly pulled off. The adhesion result was qualitatively evaluated using the criteria in ASTM D3359-17.

3. RESULTS AND DISCUSSION

3.1 Contact angle measurement

The average contact angles of the treatments were reflected in Table 1. The results were subjected to Main Effects ANOVA using the trial and treatment as independent variables and showed that there is a significant difference between the mean contact angle of the different treatments. A partial eta-squared of 0.42 also revealed that the treatments have a large effect on the difference of the mean contact angles. Using the Tukey HSD test for the post-hoc procedure, the mean contact angles of C20A treatments were not significantly different from each other. The contact angle of PS(9) was found to be significantly higher than that of C20A(3) and C20A(1) while the contact angle of the Commercial was found to be significantly higher from C20A(1) but not from C20A(3) and C20A(5).

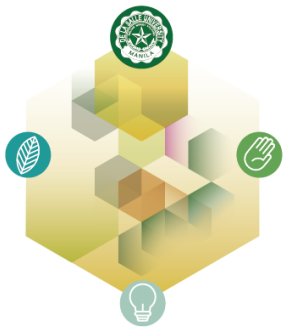

Table 1. Contact Angle Measurement Results

Treatment	Average Contact Angle (°)
Blank	84.84
Commercial	81.46
PS(9)	87.02
C20A(1)	72.23
C20A(3)	77.95
C20A(5)	79.66

3.2 Immersion test

Two parameters were used to determine the efficacy of each treatment in terms of corrosion inhibition. These are corrosion rate (C_R), in mm y^{-1}, and corrosion inhibition efficiency ($\eta\%$). The immersion test results are summarized in Table 2.

Table 2. Immersion Test Results

Treatment	Average C_R ($mm\ y^{-1}$)	Average $\eta\%$
Blank	0.06818	N/A
Commercial	0.02909	57.33
PS(9)	0.04130	39.42
C20A(1)	0.03154	53.74
C20A(3)	0.03033	55.51
C20A(5)	0.02326	65.88

The corrosion rate was computed from Eq. 1:

$$C_R = \frac{KW}{ATD} \qquad \text{(Eq. 1)}$$

where:

K = constant (8.76×10^{-4})
W = weight loss (g)
A = total surface area (cm^2)
T = time of exposure (h)
D = density of metal panel ($g\ cm^{-3}$)

The corrosion inhibition efficiency was computed through Eq. 2:

$$\eta\% = \frac{C_R - C_{R0}}{C_R} \times 100 \qquad \text{(Eq. 2)}$$

where:

C_R = corrosion rate of coated sample
C_{R0} = average corrosion rate of blank samples

The average C_R *and* % of the different treatments were subjected to One-Way ANOVA at CI=95%. It indicated that there are significant differences among the treatments in terms of both corrosion rate and corrosion inhibition efficiency. Partial eta-squared values of 0.99 and 0.95 suggest that the kind of treatment has a large effect on the C_R *and* % respectively. Post-hoc treatment of the corrosion data suggests that the average C_R of Commercial, C20A(1), and C20A(3) are comparable and not significantly different from each other, while the C_R of C20A(5), PS(9), and Blank are significantly different from other treatments. The post-hoc findings of the C_R and the % are the same.

The corrosion rate and corrosion inhibition efficiency results demonstrate that PS-only coating yields a significant difference in the corrosion rate compared to the Blank. The addition of C20A to PS can significantly decrease the corrosion rate of the metal substrates even further. At 1- and 3-wt%, the C20A treatments have similar capabilities to the commercial primer. Further increasing the composition of C20A to 5-wt% yields the best corrosion inhibition results.

According to Navarchian, Joulazadeh, and Karimi (2014) and Huttunen-Saarivirta et al. (2013), the functionalization of epoxy-based coating with organo-modified nanoclay resulted in better corrosion protection during immersion test which correlates to the improved microstructure of the polymer film and the successful exfoliation of the nanoclay in the polymer matrix. In this study, the addition of 5% C20A gave rise to a significant increase in the corrosion inhibition efficiency of the PS-based coating. This could be attributed to the improved barrier properties due to the successful incorporation of the nanoclay in the PS matrix.

3.3 Cross-hatch adhesion test

The adhesion test results were rated in accordance with the qualitative scale illustrated in ASTM-D3359-17. It was found that both 5% C20A and the commercial sample have strong adhesion properties as no peeling of the paint was observed. However, the opposite can be said for both 1% C20A and PS(9) wherein the coating was completely delaminated.

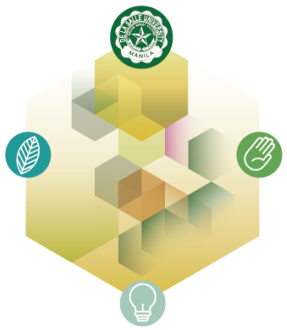

Table 3. Cross-hatch Adhesion Test Results Rated According to Criteria in ASTM-D3359-17

Treatment	*Adhesion Test Rating*		
	Trial 1	Trial 2	Average
Commercial	5B	5B	5B
PS(9)	0B	0B	0B
C20A(1)	0B	0B	0B
C20A(3)	2B	4B	3B
C20A(5)	5B	5B	5B

4. CONCLUSIONS

The researchers were able to prepare a corrosion-resistant PS-based coating modified with 5% C20A via solution-casting with D-limonene. The nanoclay was able to significantly increase the corrosion inhibition efficiency of PS-only coating which could be attributed to the enhanced barrier properties after the embedding of C20A in the PS matrix. Results also showed that C20A(5) has a significantly higher $\eta\%$ than the commercial epoxy primer. However, incorporating C20A in the PS coating resulted in a lower contact angle that increases with increasing concentration. On the other hand, the 5% C20A has excellent adhesion properties comparable to that of the commercial epoxy primer. All the while, the PS-only coating exhibited poor adhesion along with 1% C20A. These findings suggest that the optimized barrier characteristic via the successful incorporation of the nanoclay in the coating and strong adhesion properties are responsible for the corrosion protection performance of 5% C20A.

5. ACKNOWLEDGMENTS

The researchers would like to express their gratitude towards the De La Salle University Research & Grants Management Office (DLSU RGMO) for making this study possible under Fund 05 IR 1TAY19–2TAY20. Recognition also is given to Mr. Emmanuel Punzalan for his aid in solution-casting and contact angle measurement, and Dr. Retchel Arcilla for providing assistance in the statistical treatment of data.

6. REFERENCES

Ahmad, Z. (2006). Principles of Corrosion Engineering and Corrosion Control. In *Principles of Corrosion Engineering and Corrosion Control*. Elsevier Science & Technology Books. https://doi.org/10.1016/B978-0-7506-5924-6.X5000-4

Akhavan-Mahdavi, S., Sadeghi, R., Faridi Esfanjani, A., Hedayati, S., Shaddel, R., Dima, C., Malekjani, N., Boostani, S., & Jafari, S. M. (2022). Nanodelivery systems for D-limonene; techniques and applications. *Food Chemistry, 384*(August 2021), 132479. https://doi.org/10.1016/j.foodchem.2022.132479

Amr, I. T., Al-Amer, A., Selvin, T. P., Al-Harthi, M., Girei, S. A., Sougrat, R., & Atieh, M. A. (2011). Effect of acid-treated carbon nanotubes on mechanical, rheological and thermal properties of polystyrene nanocomposites. *Composites Part B: Engineering, 42*(6), 1554–1561. https://doi.org/10.1016/j.compositesb.2011.04.013

Dimitry, O.I.H., Mansour, N.A., & Saad, A.L.G. (2016). Influence of organic modifier loading on particle dispersion of biodegradable polycaprolactone/montmorillonite nanocomposites. *International Journal of Chemical and Molecular Engineering*, *10*(2), 283-297.

Firdaus, M.Y., Octaviani, H., Herlini, H., Fatimah, N., Mulyaningsih, T., Fairuuz, Z., & Bayu, A. (2021). Review: The comparison of clay modifier (Cloisite types) in various epoxy-clay nanocomposite synthesis methods. *Mediterranean Journal of Chemistry*, *11*(1), 54-74. http://dx.doi.org/10.13171/mjc02101071553myf

Fu, X., & Qutubuddin, S. (2000). Synthesis of polystyrene-clay nanocomposites. *Materials Letters, 42* (1), 12–15. https://doi.org/10.1016/S0167-577X(99)00151-2

García, M. T., Duque, G., Gracia, I., De Lucas, A., & Rodríguez, J. F. (2009). Recycling extruded polystyrene by dissolution with suitable solvents. *Journal of Material Cycles and Waste Management, 11*(1), 2–5. https://doi.org/10.1007/s10163-008-0210-8

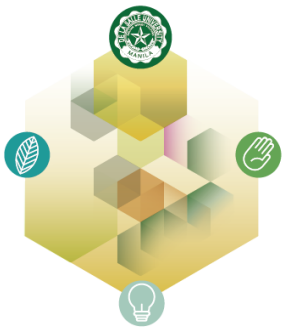

Geyer, R. (2020). Production, use, and fate of synthetic polymers. In *Plastic Waste and Recycling*. Elsevier Inc. https://doi.org/10.1016/b978-0-12-817880-5.00002-5

Gil-Jasso, N. D., Segura-González, M. A., Soriano-Giles, G., Neri-Hipolito, J., López, N., Mas-Hernández, E., Barrera-Díaz, C. E., Varela-Guerrero, V., & Ballesteros-Rivas, M. F. (2019). Dissolution and recovery of waste expanded polystyrene using alternative essential oils. *Fuel, 239*(March 2018), 611–616. https://doi.org/10.1016/j.fuel.2018.11.055

Ho, B. T., Roberts, T. K., & Lucas, S. (2018). An overview on biodegradation of polystyrene and modified polystyrene: the microbial approach. *Critical Reviews in Biotechnology, 38*(2), 308–320. https://doi.org/10.1080/07388551.2017.1355293

Huttunen-Saarivirta, E., Vaganov, G. V, Yudin, V. E., & Vuorinen, J. (2013). Characterization and corrosion protection properties of epoxy powder coatings containing nanoclays. *Progress in Organic Coatings, 76*(4), 757–767. https://doi.org/10.1016/j.porgcoat.2013.01.005

Kik, K., Bukowska, B., & Sicińska, P. (2020). Polystyrene nanoparticles: Sources, occurrence in the environment, distribution in tissues, accumulation and toxicity to various organisms. *Environmental Pollution, 262*. https://doi.org/10.1016/j.envpol.2020.114297

National Center for Biotechnology Information (2023). PubChem Compound Summary for CID 440917, D-Limonene. Retrieved August 21, 2022 from https://pubchem.ncbi.nlm.nih.gov/compound/D-Limonene.

Naderi-Samani, H., Shoja Razavi, R., Loghman-Estarki, M.R., Ramazani, M., Barekat, M., Mishra, A.K., Fattahi, H. (2019). The effects of cloisite 20A content on the adhesion strength and corrosion behavior of poly (amide-imide)/cloisite nanocomposite coatings. *Composites Part B: Engineering, 175*. https://doi.org/10.1016/j.compositesb.2019.107154

Navarchian, A. H., Joulazadeh, M., & Karimi, F. (2014). Investigation of corrosion protection performance of epoxy coatings modified by polyaniline/clay nanocomposites on steel surfaces. *Progress in Organic Coatings, 77*(2), 347–353. https://doi.org/10.1016/j.porgcoat.2013.10.008

Nazari, M. H., Zhang, Y., Mahmoodi, A., Xu, G., Yu, J., Wu, J., & Shi, X. (2022). Nanocomposite organic coatings for corrosion protection of metals: A review of recent advances. *Progress in Organic Coatings, 162*(October 2021), 106573. https://doi.org/10.1016/j.porgcoat.2021.106573

Procópio, Luciano (2019). The role of biofilms in the corrosion of steel in marine environments. *World Journal of Microbiology and Biotechnology, 35*(5), 73–. doi:10.1007/s11274-019-2647-4

Ravichandran, C., Badgujar, P. C., Gundev, P., & Upadhyay, A. (2018). Review of toxicological assessment of D-limonene, a food and cosmetics additive. *Food and Chemical Toxicology, 120*(February), 668–680. https://doi.org/10.1016/j.fct.2018.07.052

Regalado, R. J. J. M., Punzalan, E. A., & Penaloza, D. P. J. (2019). One-pot preparation of PS/silica hydrophobic coating by solution-casting using D-limonene as dispersing medium. *Epitoanyag - Journal of Silicate Based and Composite Materials, 71*(3), 80–83. https://doi.org/10.14382/epitoanyag-jsbcm.2019.14

Sales, J.N., Silva, A.A., Valenzuela-Diaz, F.R., & Moura, E.A.B. (2015). Influence of the nanoclay Cloisite 20A incorporation of properties of acrylonitrile butadiene styrene (ABS). *Characterization of Minerals, Metals, and Materials*. 159-163. 10.1007/978-3-319-48191-3_20.

Schweitzer, P. A. (2006). Paint and Coatings: Applications and Corrosion Resistance. *CRC Press*. https://doi.org/10.1201/9781351072854-6

Shikata, S., Watanabe, T., Hattori, K., Aoyama, M., & Miyakoshi, T. (2011). Dissolution of polystyrene into cyclic monoterpenes present in tree essential oils. *Journal of Material Cycles and Waste Management, 13*(2), 127–130. https://doi.org/10.1007/s10163-011-0005-1